Supplementary Information

Tumor-Specific Imaging through Progression Elevated Gene-3 Promoter-Driven Gene Expression

Hyo-eun C. Bhang[1], Kathleen L. Gabrielson[2], John Laterra[3,4], Paul B. Fisher[5], Martin G. Pomper[1,6]

[1]Department of Pharmacology and Molecular Sciences, [2]Department of Molecular and Comparative Pathobiology, [3]Department of Neurology, Johns Hopkins Medical Institutions, Baltimore, Maryland, 21231, USA, [4]Kennedy Krieger Institute, Baltimore, Maryland, 21205, USA, [5]Department of Human and Molecular Genetics, VCU Institute of Molecular Medicine, VCU Massey Cancer Center, Virginia Commonwealth University School of Medicine, Richmond, Virginia, 23298, USA, [6]Russell H. Morgan Department of Radiology and Radiological Science, Johns Hopkins Medical Institutions, Baltimore, Maryland, 21231, USA .

Address correspondence to: Martin G. Pomper, M.D., Ph.D.
Johns Hopkins Medical Institutions
1550 Orleans Street, 492 CRB II
Baltimore, MD 21231
Phone: 410-955-2789
Fax: 443-817-0990
Email: mpomper@jhmi.edu

Supplementary methods

Quantitative real time PCR. Total DNA was extracted from the snap-frozen lung tissue (For **Supplementary Fig. 5**) or fresh unfrozen tissues (For **Supplementary Fig. 8**) by using DNeasy Blood & Tissue Kit (Qiagen) with RNase A treatment to prevent mRNA contamination following the manufacturer's instruction. We used 100 ng of purified total DNA from each animal as a template. A 20 base pair-long primer set was designed to amplify 230 base pairs in the Luc encoding region in pPEG-Luc. The sequences of the primers are: 5'-TCA AAG AGG CGA ACT GTG TG-3' for Luc forward primer and 5'-GGT GTT GGA GCA AGA TGG AT-3' for Luc reverse primer. Quantitative real time PCR was performed in triplicate per template using Power SYBR® Green PCR Master Mix (Applied Biosystems). Reaction conditions were set as 50 °C for 2 min, 95 °C for 10 min and 50 cycles of 95 °C for 15 s, 60 °C for 1 min followed by the disassociation step of 95 °C for 15 s, 60 °C for 15 s, 95 °C for 15 s in a 7900HT Fast Real-Time PCR System (Applied Biosystems). Serially diluted pPEG-Luc (30.30303, 3.030303, 0.30303, 0.030303, 0.00303, 0.000303, 0.0000303, 0.00000303, 0.000000303 ng) was used as template to generate the standard curve of C_T versus log(ng total pDNA). The data were analyzed by the absolute quantification method using a standard curve by SDS v2.3 software (Applied Biosystems).

a

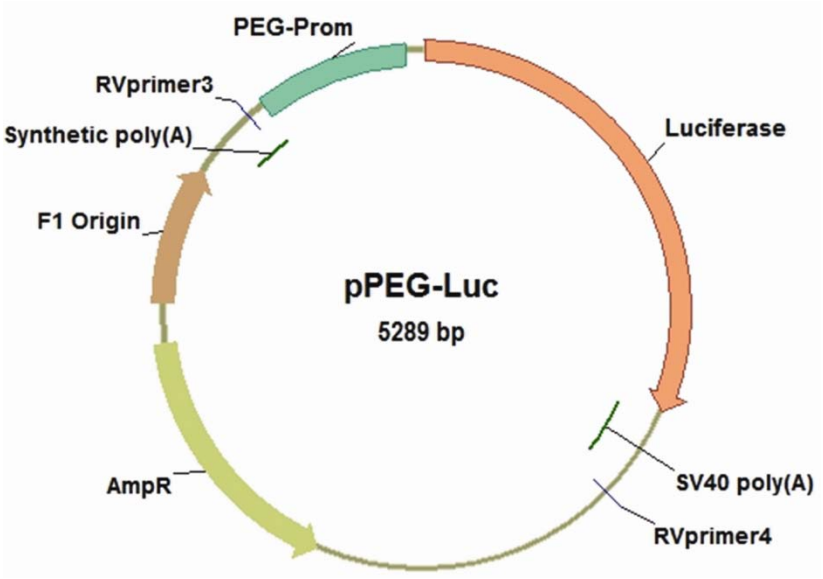

b

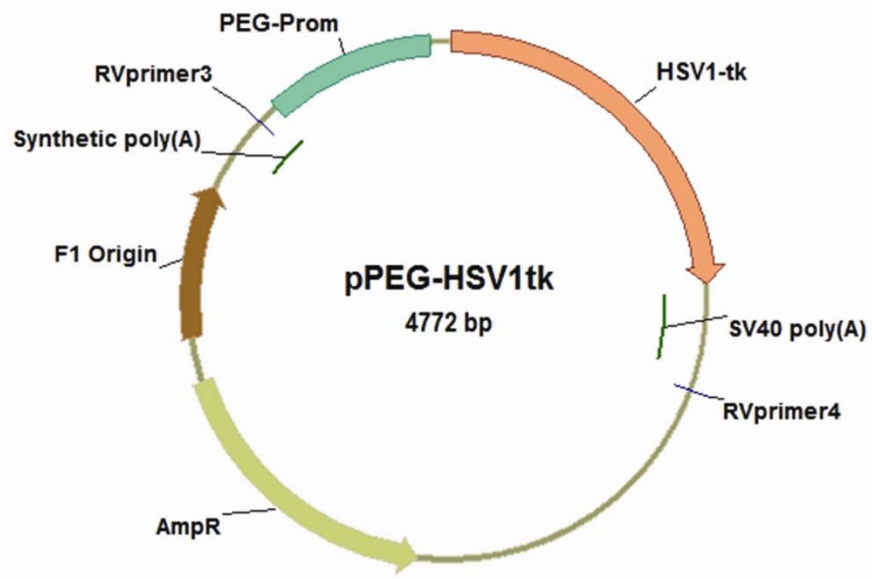

Supplementary Figure 1. PEG-Prom mediated reporter expression systems.
(**a**) Construct map of pPEG-Luc containing the firefly luciferase (Luc) encoding gene under the control of PEG-Prom. (**b**) Construct map of pPEG-HSV1tk with the HSV1-TK encoding gene downstream of PEG-Prom.

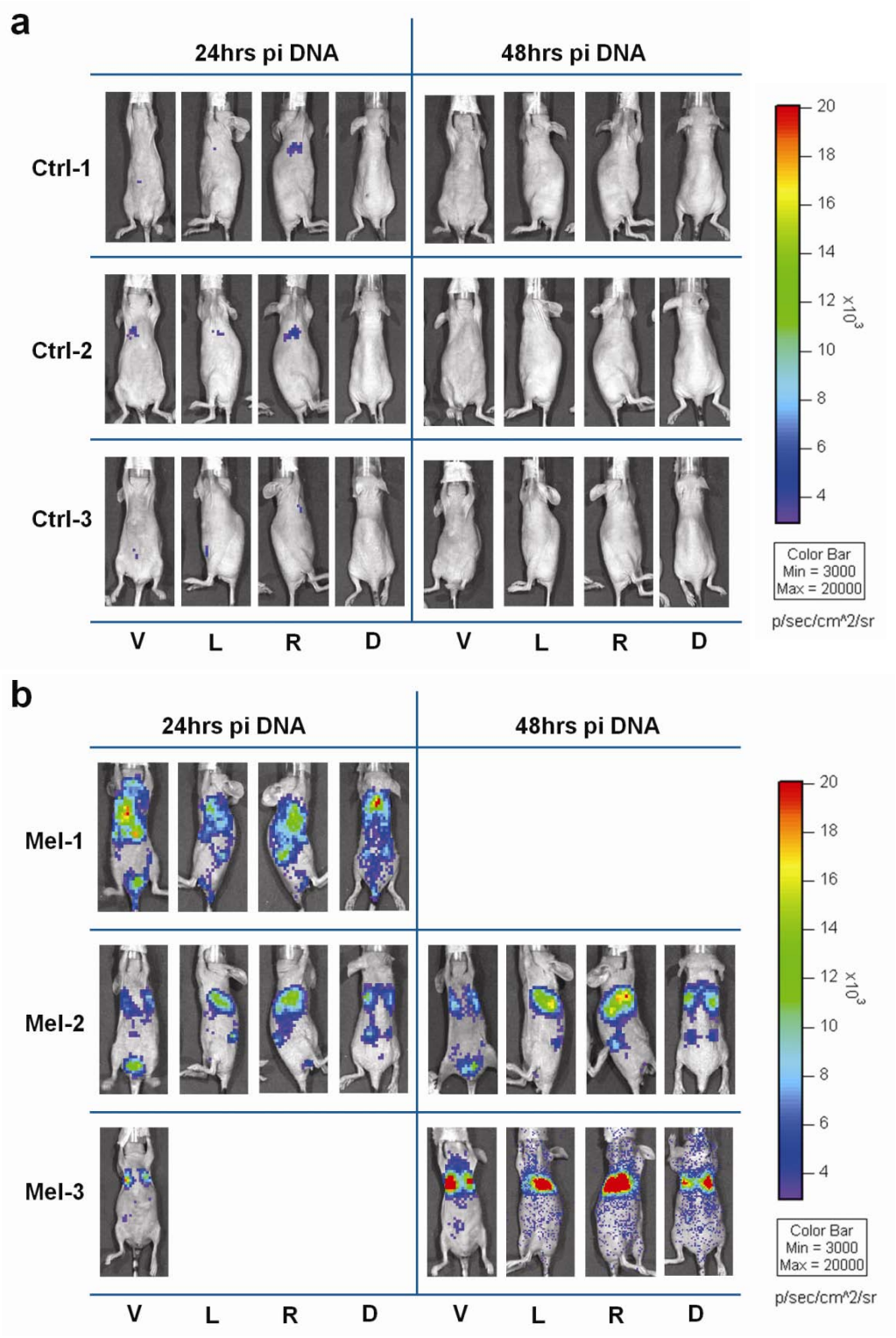

Supplementary Figure 2. Cancer-selective PEG-Prom activity shown by bioluminescence imaging (BLI) in an experimental model of human melanoma metastasis (Mel). (**a**) BLI showing Luc expression in the control group of healthy mice (*n* = 3; Ctrl-1–3). (**b**) BLI showing Luc expression observed in the Mel group (*n* = 3; Mel-1–3). The images were acquired at 24 and 48 h after the intravenous (IV) delivery of pPEG-Luc/PEI polyplex. Each animal was imaged from four directions (V, ventral; L, left side; R, right side; D, dorsal views). Pseudo-color images of the two groups are adjusted to the same threshold values. Bioluminescent signal was observed specifically in the Mel models at both time points. (Mel-1 did not survive until the 48 h time point.)

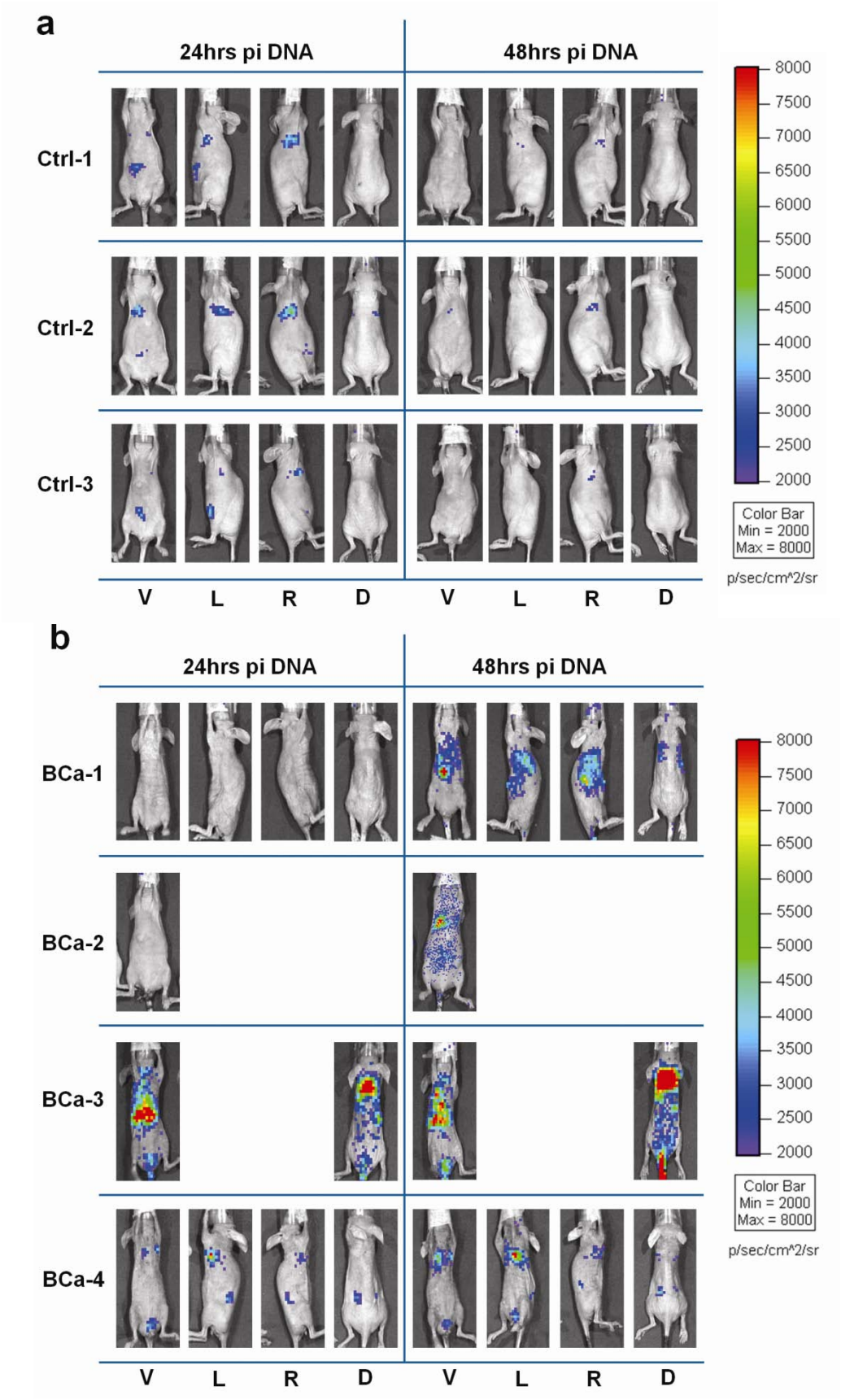

Supplementary Figure 3. Cancer-specific PEG-Prom activity shown by BLI in an experimental human breast cancer metastasis model (BCa). (**a**,**b**) BLI of the control group (**a**, *n* = 3; Ctrl-1–3) and the BCa group (**b**, *n* = 4; BCa-1–4). Images were acquired at 24 and 48 h after the IV delivery of pPEG-Luc/PEI polyplex. Each mouse was imaged from four directions (V, ventral; L, left side; R, right side; D, dorsal views). Pseudo-color Images of the two groups are adjusted into the same color scale.

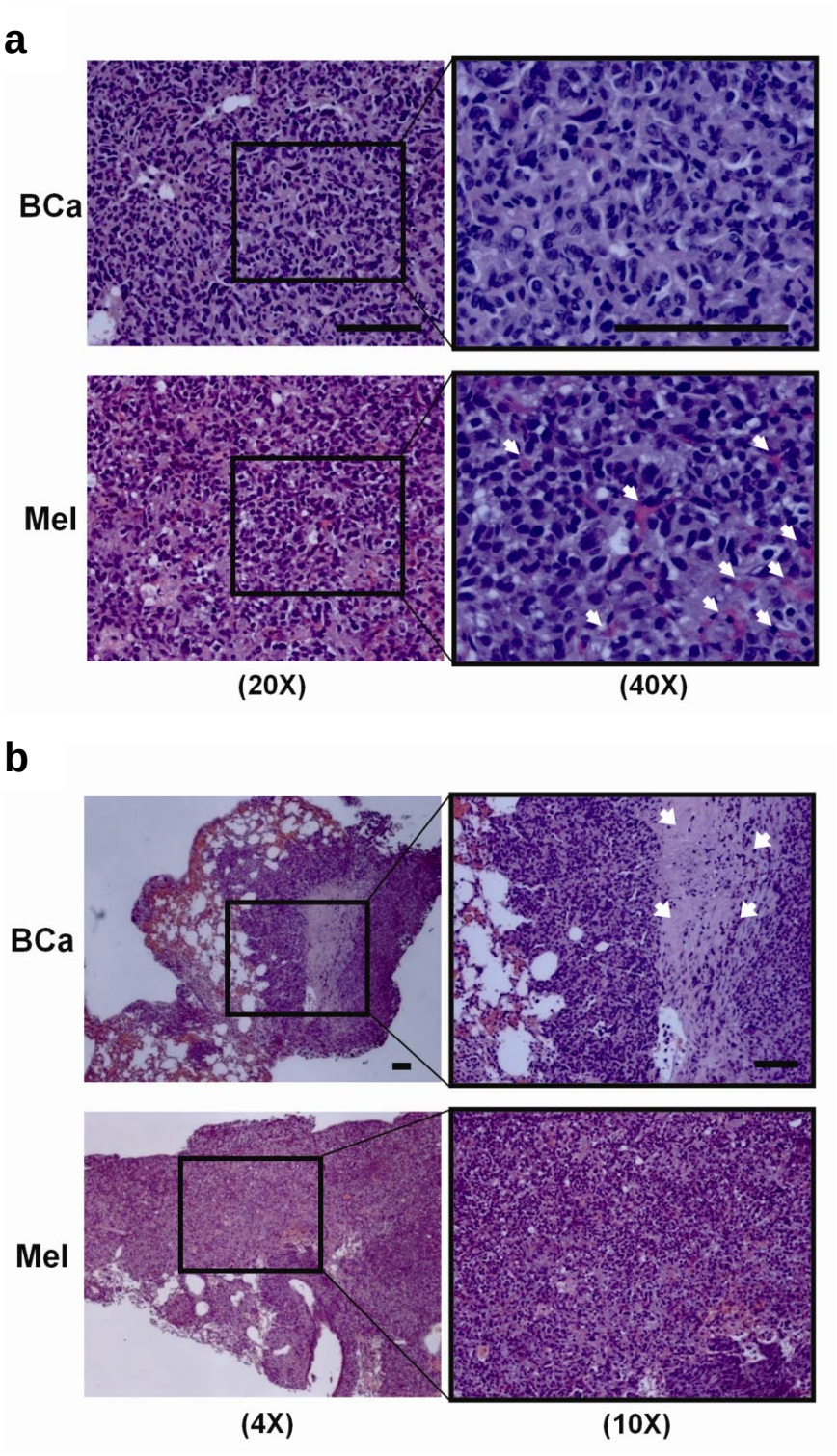

Supplementary Figure 4. Hematoxylin and eosin (H&E) staining of formalin-fixed, paraffin-embedded (FFPE)-lung sections from experimental metastasis models of human melanoma (Mel) and breast cancer (BCa). (**a**) Representative images of lung sections from a BCa and a Mel mouse model. The lung was extracted approximately 6 weeks after the intravenous injection of MDA-MB-231 (for BCa) or MeWo (for Mel) cell lines. When we compared metastatic nodules with similar cancer cell density found in BCa and Mel, the histological analysis demonstrated significantly higher vascularization in Mel than BCa (white arrows in Mel-40X). (**b**) Representative images of the lung sections with lower magnification. While MeWo cells were widely dispersed in the whole lung lobe in Mel, MDA-MB-231 cells formed a largely concentrated tumor, which resulted in a necrotic center (white arrows in BCa-10X). Scale bars, 100 μm.

a

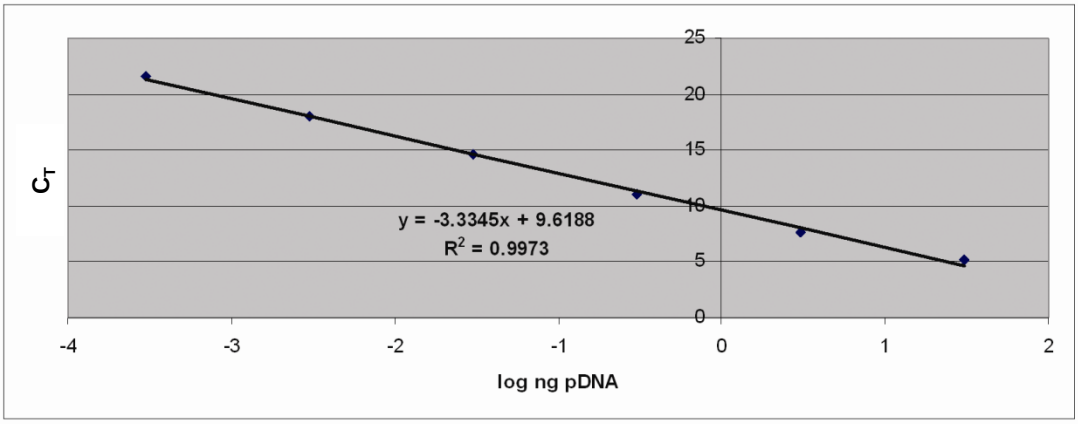

b

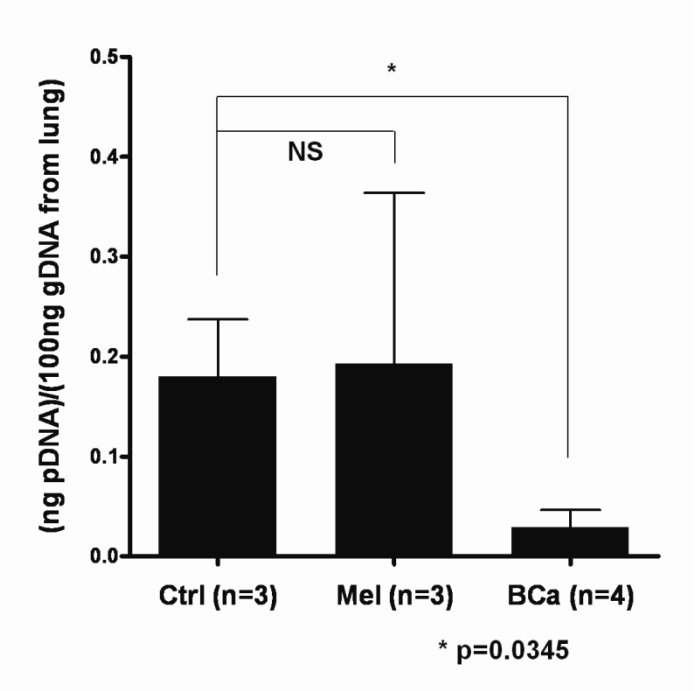

Supplementary Figure 5. Intergroup comparison of the gene delivery efficiency to lungs. After 48 h BLI session, the absolute amount of pPEG-Luc in lung tissues of each animal was quantified by quantitative real time PCR. (**a**) Standard curve plot of C_T value versus log ng pDNA (pPEG-Luc). (**b**) Absolute quantification of the pDNA delivery efficiency to lungs using the standard curve method. While no significant difference was observed between the control and the experimental models of human melanoma metastasis (Mel), the breast cancer metastasis models (BCa) had significantly lower transfection efficiency compared to the control. Error bars represent means ± s.e.m. (*n* = 3 for Ctrl; *n* = 3 for Mel; *n* = 4 for BCa) (NS, no significant difference; * *p* = 0.0345)

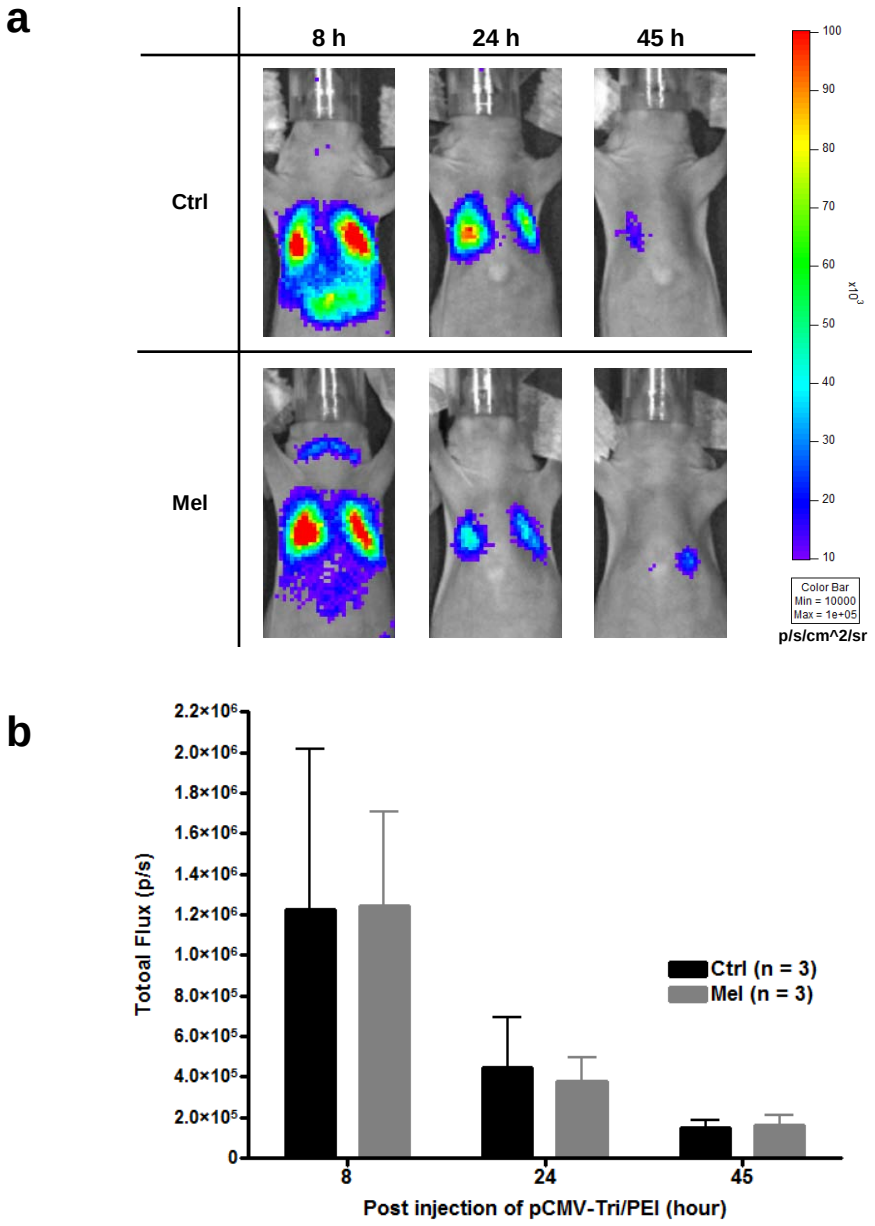

Supplementary Figure 6. Comparison of constitutive CMV promoter activity in the healthy control (Ctrl) and experimental melanoma metastasis (Mel) groups. (**a**) Serial BLI of one representative animal from the Ctrl and Mel groups. The images were acquired at 8, 24 and 45 h after the systemic delivery of pCMV-Tri/PEI polyplex. The animal model and pDNA/PEI polyplex were generated as described in **Methods**. Pseudo-color images of the two groups are adjusted to the same threshold values. (**b**) Quantification of bioluminescent signal intensity measured in ROIs drawn over the thoracic cavity of the animals. No significant difference in the CMV promoter activity was observed between the Ctrl and Mel groups at any time points. Error bars represent means ± s.e.m. (*n* = 3 for Ctrl; *n* = 3 for Mel)

BCa-1

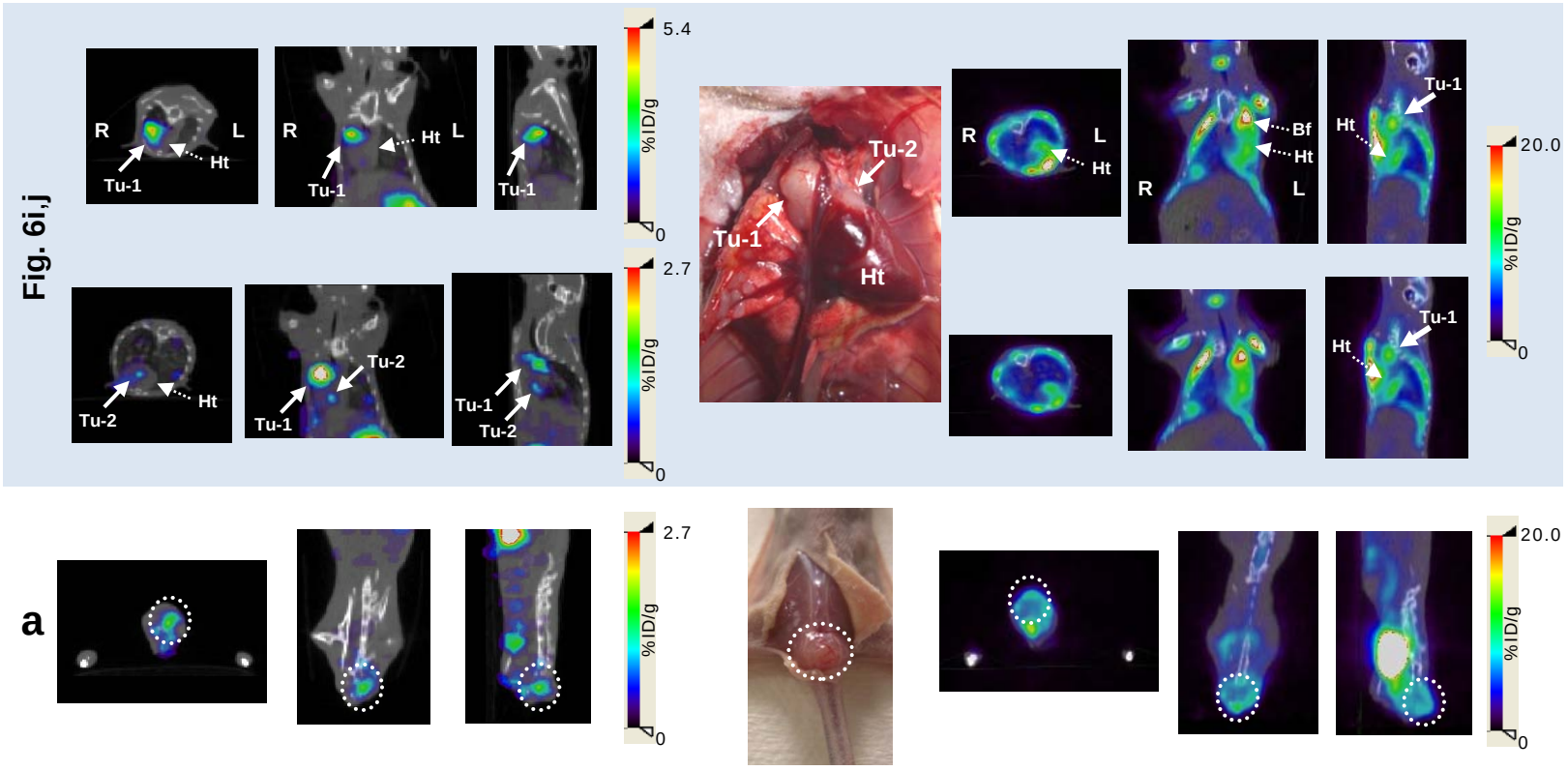

Mel-6

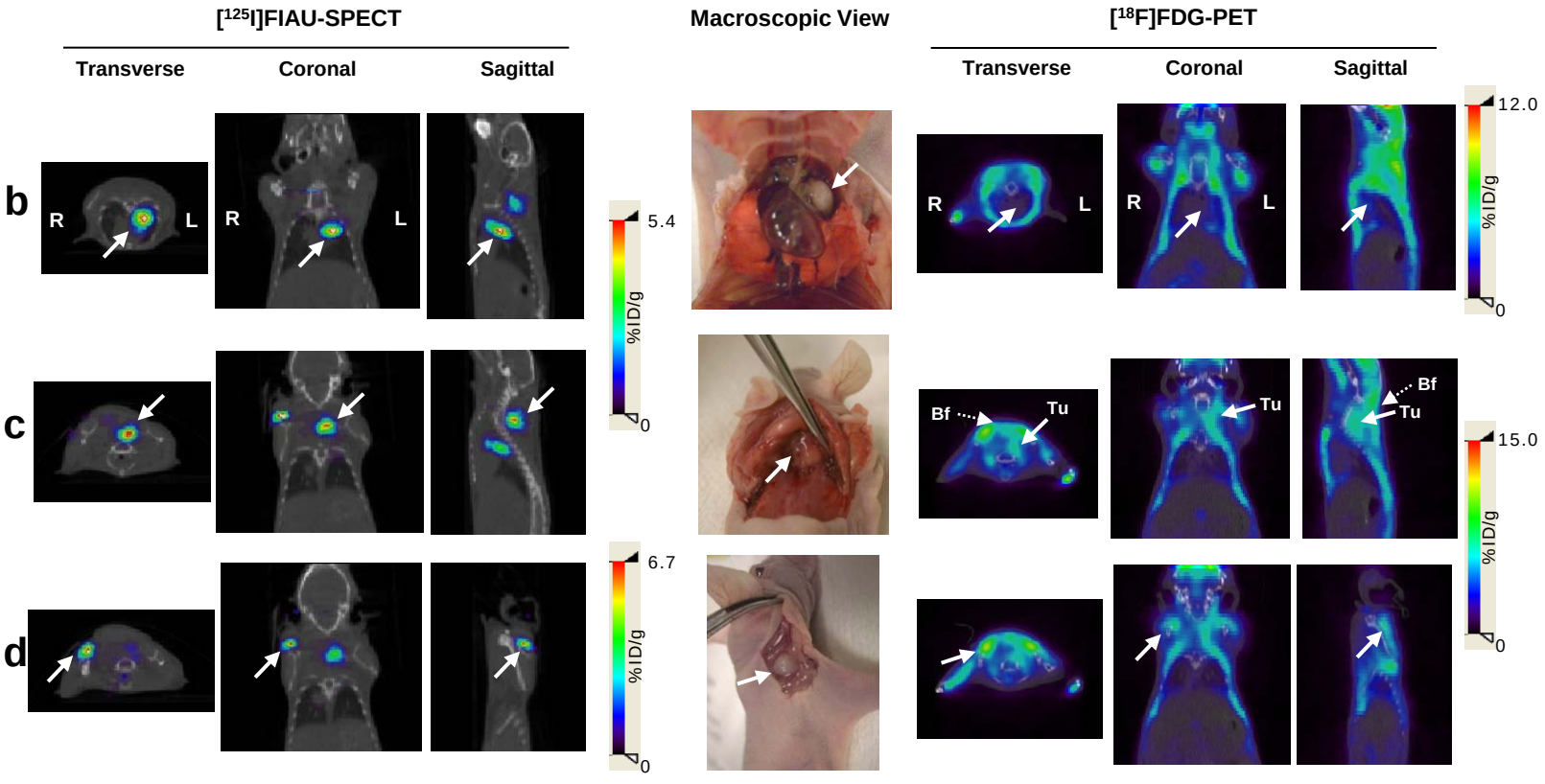

Supplementary Figure 7.

Mel-7

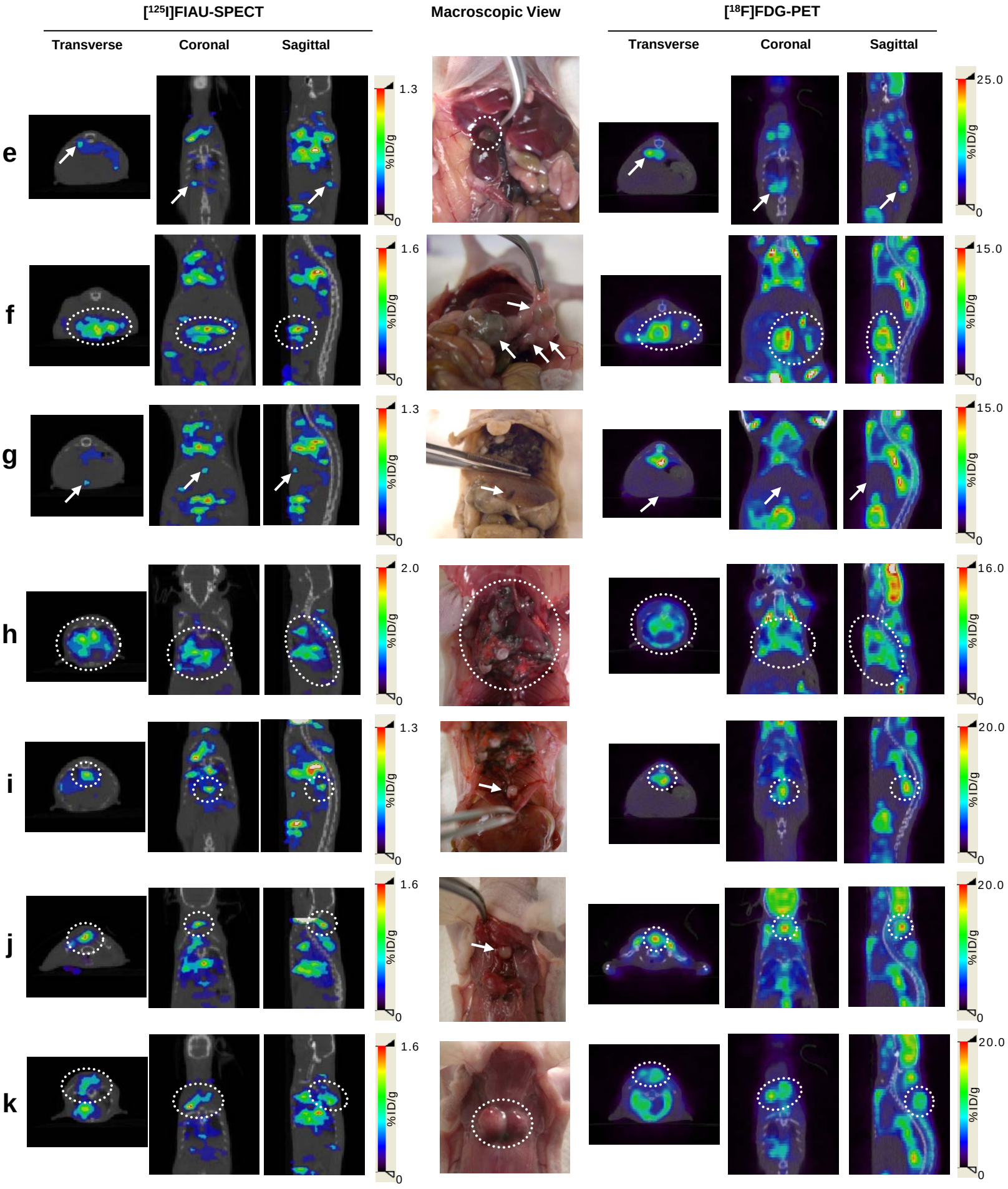

Supplementary Figure 7.

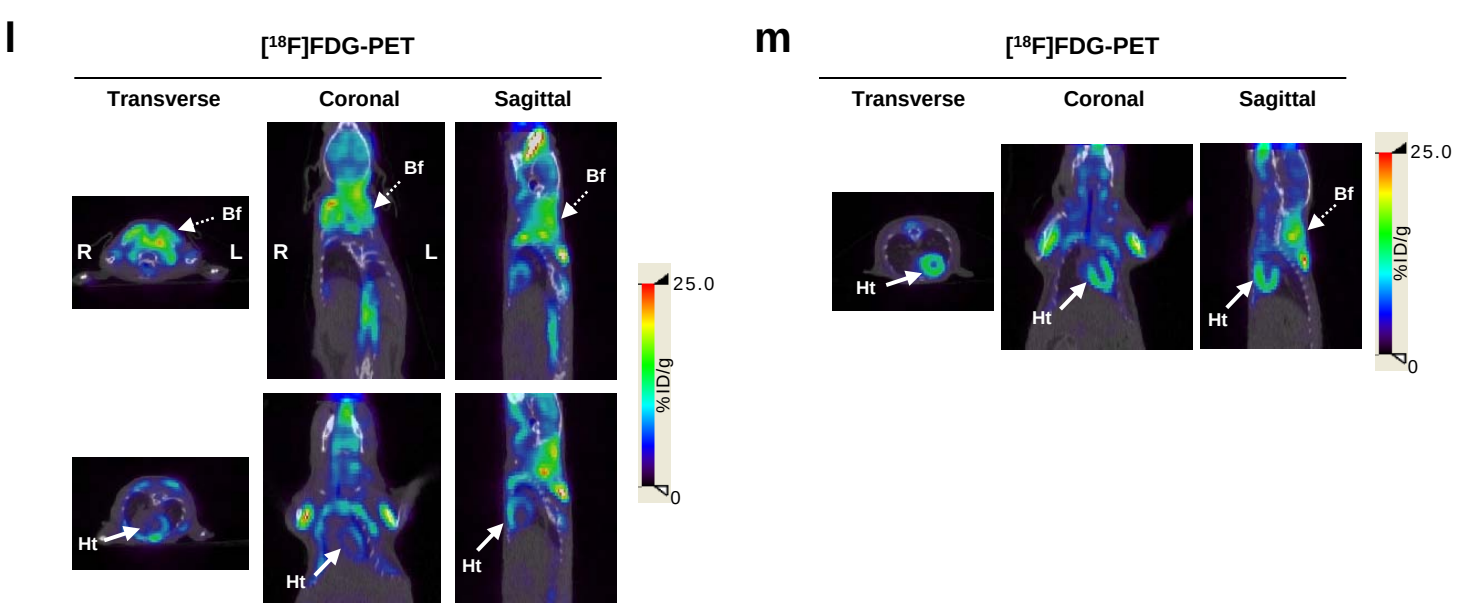

Supplementary Figure 7. Cross-comparison of detection accuracy between the PEG-Prom-mediated imaging systems and conventional [^{18}F]FDG-PET in the experimental metastasis models, BCa and Mel. (**a**) SPECT and PET images of a representative animal from the BCa group, BCa-1. In addition to the two nodules found adjacent to the heart (**Fig. 5i**,**j**), one mass was detected on the dorsal surface of the base of the tail by both [^{125}I]FIAU-SPECT and [^{18}F]FDG-PET. (**b**—**d**) SPECT and PET images of a representative animal from the Mel group, Mel-6. By [^{125}I]FIAU-SPECT, three tumor masses were found in the rib cage close to the heart and the left lung (**b**), under the brown fat (**c**) and presumably in the salivary gland (**d**), which were confirmed by gross pathologic examination. The latter two tumors were also detected by [^{18}F]FDG-PET (**c**,**d**) even though the signal-to-background ratio was too high to differentiate the tumors clearly. (**e**—**k**) SPECT and PET images of Mel-7. In most cases, the imaging results were well correlated between [^{125}I]FIAU-SPECT and [^{18}F]FDG-PET imaging. Both techniques detected metastatic sites in the right adrenal gland (**e**), in the pancreas (**f**), in the right and left lung lobes (**h**), on the dorsal thoracic wall right above the diaphragm (**i**) and under the brown fat (**j**,**k**). Exceptionally, a small nodule on the surface of the liver confirmed by necropsy was detected by [^{125}I]FIAU-SPECT, but not by [^{18}F]FDG-PET (**g**). White arrows and dotted circles indicate the corresponding location in the pairs of co-registered SPECT-CT and PET-CT images. (**l**,**m**) Representative [^{18}F]FDG-PET images of two healthy control animals, Ctrl-4 and Ctrl-5. Considerable level of [^{18}F]FDG uptake was observed in the brown fat, heart and brain of the controls.

SPECT images were acquired 48 h post injection of [^{125}I]FIAU which was 94 h after the pPEG-HSV1tk/PEI delivery. PET images were acquired 1 h post injection of [^{18}F]FDG. For BCa-1, PET imaging was performed on the last day of SPECT imaging. For Mel-6 and Mel-7, PET scans were done two days prior to the pPEG-HSV1tk/PEI injection. pPEG-HSV1tk/PEI and [^{18}F]FDG injections were done with five (BCa-1) and three day-intervals (Mel-6 and Mel-7) to perform the two imaging studies as close as possible, considering the different energy window and half-life of F-18 and I-125. (Tu, tumor; Ht, heart; Bf, brown fat)

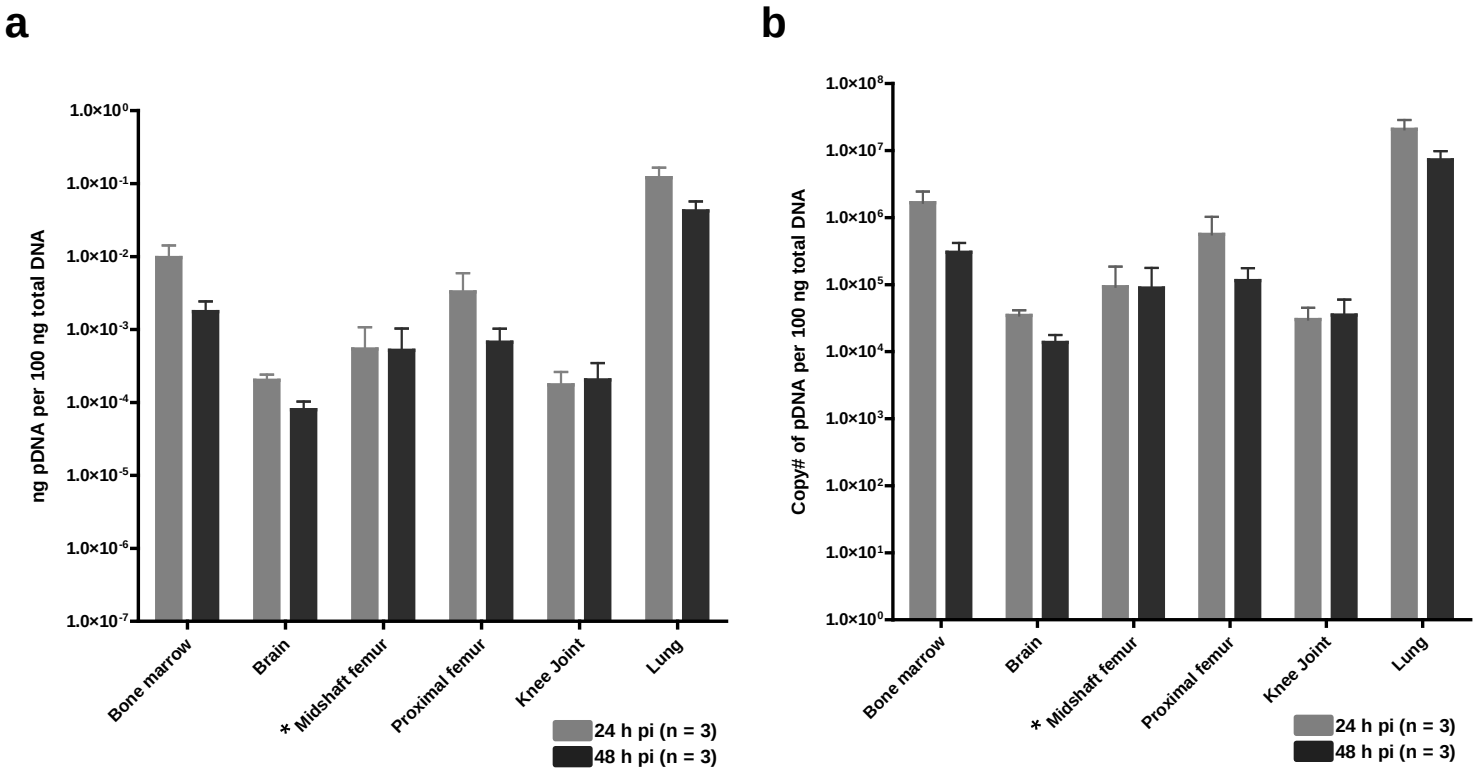

Supplementary Figure 8. Evaluation of pDNA transfection efficiency to bone and brain through the in vivo-jetPEI^{TM}-mediated systemic delivery. (**a**,**b**) Absolute quantitation of the amount of pDNA delivered to bone and brain by using quantitative real time PCR using the standard curve. Twenty four and 48 h after the systemic delivery of pPEG-Luc/PEI polyplex into female NCR nu/nu mice (Charles River), bone marrow, midshaft femurs, proximal femurs, knee joints and brains were collected along with lungs as a positive control, and total genomic DNA was extracted from the fresh unfrozen tissues. The absolute amount of pPEG-Luc delivered into each organ was quantified in ng pDNA (**a**) and in the pDNA copy number (**b**) per 100 ng total DNA. Error bars represent means $\pm$ s.e.m. (n = 3 per each time point) *Midshaft femur: Only the femoral midshaft cortical bones were used for total DNA extraction after the removal of bone marrow.

Supplementary Video 1. Detection of metastatic melanoma after systemic administration of pPEG-HSV1tk/PEI polyplex using SPECT-CT. Movie of a representative melanoma metastasis model, Mel-2 from **Fig. 4b** and **Fig. 5a**,**b**. The image was acquired at 24 h post injection of [^{125}I]FIAU (1.4 mCi), which was 70 h after the pPEG-HSV1tk delivery. Multiple metastatic sites are predicted in the lung and upper dorsal area of the animal by [^{125}I]FIAU SPECT. Melanoma masses were confirmed under the brown adipose tissue in the corresponding area (**Fig. 5b**) as well as in its lung by the gross pathological analysis.

Supplementary Video 2. Movie of a representative control animal, Ctrl-3 from **Fig. 4a**. This whole body SPECT-CT image was acquired at 24 h post injection of 1.4 mCi of [^{125}I]FIAU, which was 70 h after the IV injection of pPEG-HSV1tk/PEI polyplex. Accumulated radioactivity was only detected in the urinary bladder and intestines of the animal. The same pseudo color scale used for Mel-2 in **Supplementary Video 1** was applied.